國 立 交 通 大 學

電 信 工 程 學 系 碩 士 班

碩 士 論 文

積體光學電路中緩衝結構之研究

Study of Transition Structures in Integrated Optics

研 究 生 ： 羅正倫

指導教授 ： 彭松村 博士

黃瑞彬 博士

中華民國九十三年七月

積體光學電路中緩衝結構之研究

Study of Transition Structures in Integrated Optics

研 究 生:　羅正倫　　　　　　　　Student:　Cheng-Lun Lo

指導教授:　彭松村 博士　　　　　　Advisor:　Dr. Song-Tsuen Peng

　　　　　黃瑞彬 博士　　　　　　　　　　　Dr. Ruey-Bing Hwang

國立交通大學

電信工程學系碩士班

碩士論文

A Thesis

Submitted to Institute of Communication Engineering

College of Electrical Engineering and Computer Science

National Chiao Tung University

In Partial Fulfillment of the Requirements

for the Degree of

Master of Science

In

Communication Engineering

July 2004

HsinChu , Taiwan , Republic of China.

中華民國九十三年七月

積體光學電路中緩衝結構之研究

研 究 生: 羅正倫　　　　　　　　指導教授: 彭松村 博士

　　　　　　　　　　　　　　　　　　　　黃瑞彬 博士

國立交通大學電信工程學系碩士班

摘　　要

　　由於現在光學積體電路的尺寸不斷地在縮小，為了使能量能有效地傳輸，電路內部用於緩衝的介質波導其設計就顯得更加地重要。我們整篇的文章將用可分析幾乎任何形狀的階梯進似法以及波模匹配法來獲取我們所要的結果。在此，為了簡化我們複雜的問題，我們將整個結構塞進一個全尺寸的上下平行金屬板內來分析，並且把上下金屬板拉的夠開的狀況下去計算以逼近實際的物理狀況。在第三章中，我們列舉了一些典型的結構，其所得到的數據以及圖表可以做為日後要設計該緩衝介質波導時一個可依循的標準。依照我們想要的傳輸量，藉由所得的圖表，所對應結構的尺寸大小我們可以有準則地去獲得了。

Study of Transition Structures in Integrated Optics

Student: Cheng-Lun Lo   Advisor: Dr. Song -Tsuen Peng

                          Dr. Ruey -Bing Hwang

Institute of Communication Engineering

National Chiao Tung University

July 2004

Abstract

Due to the limitation on the size of an optical integrated circuit, the circuit topology should be simplified   However, to have an efficient transmission for the signal, a good design with transition structures becomes important gradually   In light of its unique and complex theoretical basis required, in this thesis, we present an systematical analysis for a class of transition structures by the rigorous mode matching method   In order to simply our sophisticated problem, we insert the overall structure into an oversized metallic parallel-plate waveguide   Furthermore, we separate the distance of the parallel-plate waveguide far enough to approximate the practical case   Finally, in the chapter 3, we illustrate several typical transition structures, and the numerical data we obtained later can be developed as a guideline while designing them   From these figures, we can easily get the size of the structure with the desired transmission efficiency

誌　謝

　　首先，我真的很謝謝我的兩位指導老師 – 彭松村教授以及 黃瑞彬教授，由於他們不厭其煩地教導我，使得這一篇論文能夠順利地完成。同時我也要感謝這兩年來陪伴我一起研究的實驗室同學以及學長們，在這兩年之中，我們相處地很愉快，使得在研究壓力頗大的研究過程中能夠得以舒展。最後，謹將此篇論文獻給我的父母，感謝他們多年來辛苦的栽培和關懷。

Acknowledgement

　　First of all, I would like to express my deepest gratitude toward two advisors of mine, Dr. Song-Tsuen Peng and Dr. Ruey-Bing Hwang . For their enthusiastic guidance and invaluable suggestions, the thesis can be finished successfully . At the same time, I am also thankful to my senior schoolmates in the same laboratory . For getting well with them, I can release the enormous stress during doing the research . Finally, I would like to show my sincere gratefulness with the thesis to my parents for their inspiration and love .

Contents

List of Figures

Chapter 1

Introduction

An optical integrated circuit (OIC) contains various types of components, such as diffraction gratings, dielectric waveguide, laser diode and etc Such that there are many interfaces present in the circuit In general, the interface between two components (or devices) exhibits the structure of discontinuity   As we have known, these discontinuities will cause enormous power leakage and reflection while wave propagating through them Moreover, due to the compact size of the OIC, such a leakage will cause more serious crosstalk between neighboring components than before, and degrade system performance   Besides, the high insertion loss due to a strong reflection from discontinuities will further reduce the performance of the system

In order to reduce the reflection caused by the junction discontinuities, the components are usually connected by smooth transition structures, such as a bended or a crack which may be considered as nonuniform waveguides Therefore, It is important to know how to design an optimal transition structure to reduce the power reflection and enhance the transmission efficiency We have extensively surveyed the guiding characteristics of uniform and nonuniform dielectric waveguides [1-6] We found that although transition structures have been studied [7] , but the profiles are limited to some specific patterns Therefore, in this thesis, we will analyze a variety of the transition structures to systematically understand the

physical picture of wave scattering from a discontinuity and to obtain the criterion for engineering design

Some typical transition structures are shown in Fig1.1 The structure in Fig1.1 (a) shows a transition between two nonaligned identical waveguides, where the thickness of the waveguide is kept at a fixed value throughout the entire structure The structure in Fig1.1 (b) shows a transition in a perturbed waveguide having a section with different thickness throughout the entire structure The structure in Fig1.1 (c) shows a transition between two uniform waveguides with different thickness, and the structure in Fig1.1 (d) shows a transition of a bended waveguide with symmetric profile
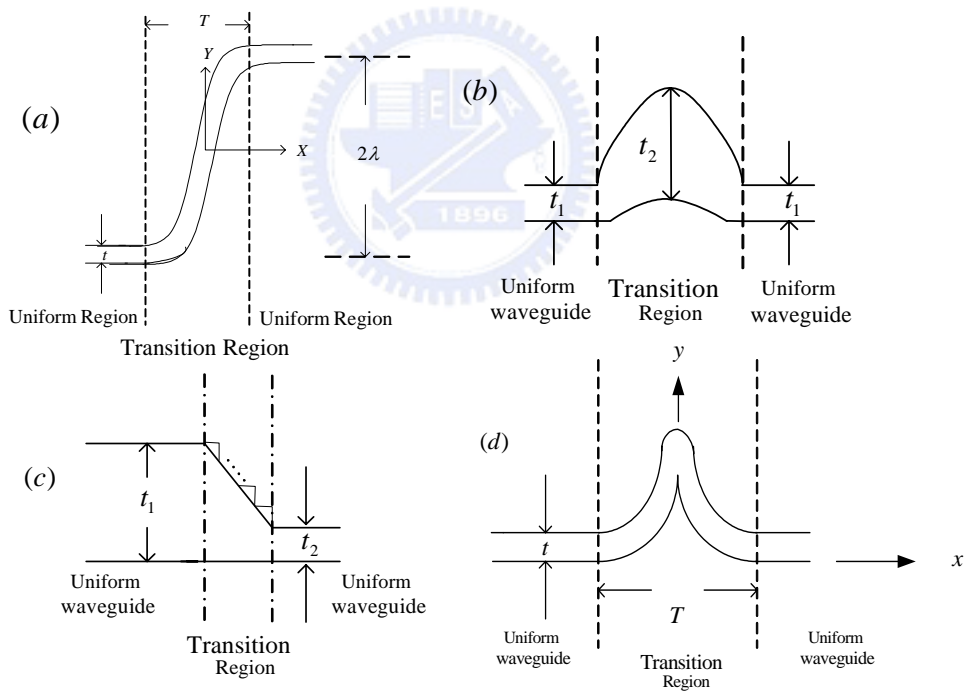
Fig1.1 Typical profiles of transition structures
(a) Bended waveguide-type A
(b) Perturbed waveguide
(c) Two nonidentical waveguides
(d) Bended waveguide-type B

It is not easy to obtain the chose-form solution for the scattering characteristics of the nonuniform open dielectric waveguides, even for simple geometrical structure   Therefore, we must take advantage of approximate procedure   In this thesis, the rigorous mode matching method was employed to deal with waveguide transition structure   Wherein, the scattering characteristic of waveguide modes by the structures having many discontinuities was carried out by computer numerical simulation

Chapter 2

Method of Analysis

━━━━━━━━━━━━━━━━

In order to simplify our analysis, we carry out two procedures here　First, we use the staircase approximation as shown in section 2.1　After putting the structure inside an over-sized parallel-plate waveguide, we have the complete set of modes in any region　Second, we analyze the problem by using the mode matching method, and thus the equivalent transmission-line network representation is obtained, which is the kernel of the entire analysis　Furthermore, the amplitudes of forward wave and backward wave in any region are determined by solving the voltage and current amplitudes in the transmission-line equations　Once they are determined, the reflection and transmission efficiencies of each mode can be understood immediately, and thus the problem is totally resolved

2.1　Staircase approximation

From Fig 2.1, we can observe that we use the staircase approximation to approximate a continuous profile　As shown in this figure, such an approximation yields the structure containing three uniform layers for each partition denoted by dash lines　Here, we use "region" to represent any partition in the structure, as is region A and region B shown in this figure

When we put the structure into an oversize parallel-plate waveguide, a complete set of modes for each region can be well established, and thus a basic equivalent network will be developed for a junction between any two adjacent regions [8-9]   Therefore, for the entire structure, we can cascade these basic unit cells to form an overall equivalent network as is described clearly later with mode matching method in section 2.2   Evidently, if we minimize the step size, the approximated structure will approach the practical one   Having such an approximation, we can not only simplify the mathematical analysis but also easily interpret the physical phenomenon of the results obtained in the next chapter
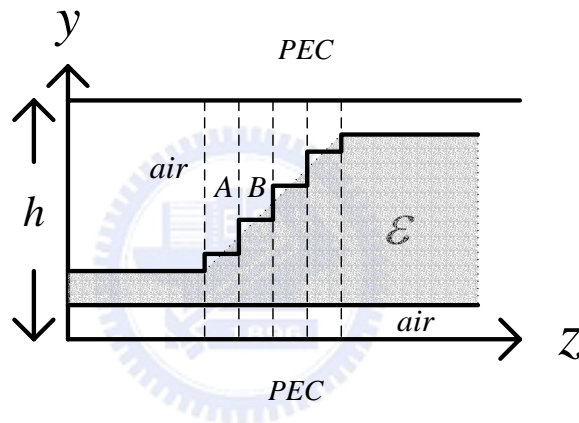
Fig 2.1   Staircase approximation of an arbitrary continuous profile

2.2 Mode matching method

In this section, we will introduce the procedures of the mode matching method in dealing with the problem described in the previous section   First, we want to find the eigen modes for a prescribed layered structure   Second, once the eigen modes are determined, the relationship between the mode amplitudes for the two adjacent regions could be determined   Finally, we will assess the magnitudes of the voltage and the current for each mode in each region by using the transfer matrices

2.2.1 Transverse-resonance technique

By imposing the condition of transverse resonance along the y direction while wave propagates in the z direction, we could set up an equation to solve the propagating wavenumber k_z and the corresponding mode function $\phi(y)$ Where k_z is defined as $\frac{2\pi}{\lambda}\sqrt{\varepsilon_{eff}}$, and ε_{eff} is the effective dielectric constant A transverse equivalent network for a parallel-plate waveguide containing three uniform layers is shown in the Fig 2.2 For TE mode, the wavenumber and the characteristic impedance along the y direction can be defined as below

$$k_y = \frac{2\pi}{\lambda}\sqrt{\mu\varepsilon_i - \varepsilon_{eff}} \quad (\mu = \mu_0) \tag{2-1}$$

$$Z_y = \frac{\omega\mu_0}{k_y} \tag{2-2}$$

Where λ is the wavelength , ε_i is the relative dielectric constant for each uniform layer ($i = d$ or a) Moreover, the condition of the resonance is defined as below

$$Z_{up} + Z_{dn} = 0 \tag{2-3}$$

Where Z_{up} and Z_{dn} are defined as the input impedance looking upward and downward from the reference plane For a given set of the structure parameters and the operating wavelength, by evaluating equation (2-3), we can easily determine the effective dielectric constants in the structure
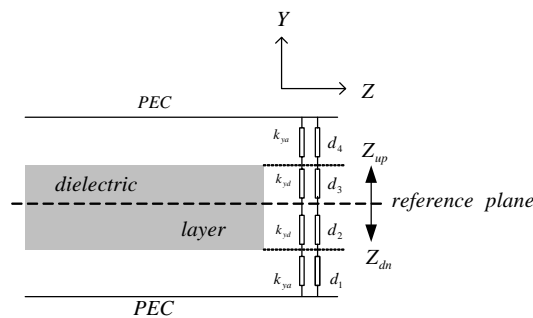

Fig 2.2 Equivalent transmission-line network for a parallel-plate waveguide containing three uniform layers

Once the roots were found, we could determine the corresponding eigen function, namely mode function $\phi(y)$, distributed in the cross section For TE mode, we can know that the mode function relates to E_x or H_y and could be written as below

$$\phi_n(y) = \begin{cases} Z_{yn,p} A_{n,p} \sin(k_{yn,p} y + \theta_{n,p}) & \text{for general layer} \\ Z_{yn,nd} A_{n,nd} \sin(k_{yn,nd}(h-y)) & \text{for the last layer} \end{cases} \qquad (2\text{-}4)$$

Where n denotes the nth mode, p represents the pth layer, $A_{n,p}$ and $\theta_{n,p}$ are the amplitude and phase of the nth mode field distributed in the pth layer, $Z_{yn,p}$ and $k_{yn,p}$ are the characteristic impedance and the wavenumber along the y direction as described previously , h is the distance between two PEC, and we assume that there are nd layer in one region

The next step is to find the value of $A_{n,p}$ and $\theta_{n,p}$ in each layer Because of the vanishment for the tangential electric field at the surface of the PEC ($E_x = 0$ at $y = 0$ and $y = h$), the $\phi_n(y)$ for the first layer has the form as shown in (2-4) with vanishing $\theta_{n,1}$ Furthermore, we set the value of $A_{n,1}$ in the first layer to be one By the electromagnetic boundary condition, that is, the tangential field components must be continuous at the interface between two adjacent dielectric layers, the general solution for the argument $\theta_{n,p}$ and the amplitude $A_{n,p}$ could be obtained, written below:

$$\theta_{n,p+1} = \tan^{-1}\left(\frac{Z_{yn,p}}{Z_{yn,p+1}} \tan(k_{yn,p} D_p + \theta_{n,p}) \right) - k_{yn,p+1} D_p \qquad (2\text{-}5)$$

$$A_{n,p+1} = A_{n,p} \frac{\cos(k_{yn,p} D_p + \theta_{n,p})}{\cos(k_{yn,p+1} D_p + \theta_{n,p+1})} \qquad (2\text{-}6)$$

and the last layer $\quad A_{n,nd} = A_{n,nd-1} \dfrac{\cos(k_{yn,nd-1} D_{nd-1} + \theta_{n,nd-1})}{\cos(k_{yn,nd} d_{nd})} \qquad (2\text{-}7)$

Where p ranges from one to nd By progressively matching the field quantity at the interfaces, we could resolve the unknown $A's$ and $\theta's$ in each region, and thus the mode function in the transverse plane for each mode can be totally determined

Since the eigen function $\phi_n(y)$ satisfies the Sturm-Liouville differential equation and the prescribed boundary condition, they should satisfy the orthogonal relation given below:

$$\left\langle \phi_m^{(i)*}(y) \middle| w(y) \middle| \phi_n^{(i)}(y) \right\rangle = \delta_{mn} \tag{2-8}$$

Where i denotes the ith region, m and n represent different mode indices, $w(y)$ is the weighting function corresponding to Sturm-Liouville differential equation For TE mode, the weighting function is defined as below

$$w(y) = 1 \tag{2-9}$$

After normalizing each $\phi_n(y)$, we can plot them as shown in the Fig 2.3 Here, we demonstrate a three uniform layers structure and plot the tansverse electric field distribution for the first six modes As shown in this figure, the field, or power density, is guided in the dielectric layer when the corresponding root is greater than unity Such a hind of mode can be regarded as surface wave in dielectric waveguide since the field component is decaying at the surrounding medium, such as air On the contrary, those with effective dielectric constant smaller than unity mean that the wave is propagating in all regions, that is, they exhibit sinusoidal variation in each constituent region

TE

three layer

8
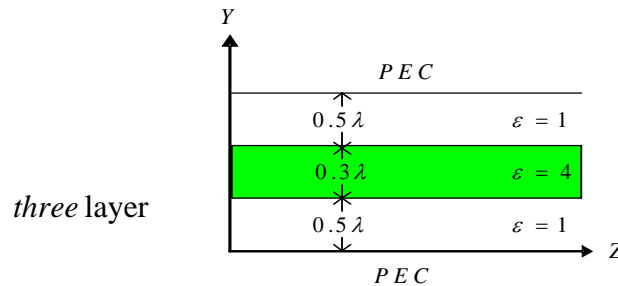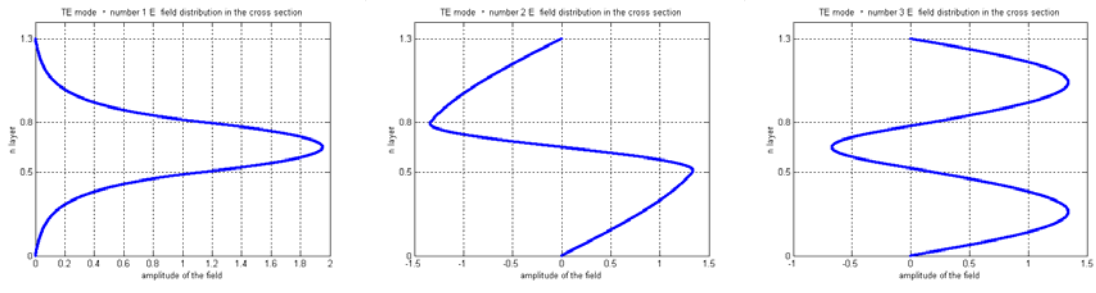
| ε_{eff} : | 2.9842 | 0.8715 | 0.0899 |

Fig 2.3   Transverse fields in a three uniform layers structure for one TE mode

2.2.2 Electromagnetic boundary conditions

After obtaining the eigen modes distributed in a multilayered structure, we shall

formulate the boundary value problem along the direction of wave propagation in order to

determine the relationship of mode amplitudes at the interface between two adjacent regions

Referring to Fig 2.4 (a), the two regions on the both sides of the discontinuity are

characterized by different distributions of the dielectric constant and a junction discontinuity is

at $z = z_0$ According to the principle of separation variable, the tangential E and H fields
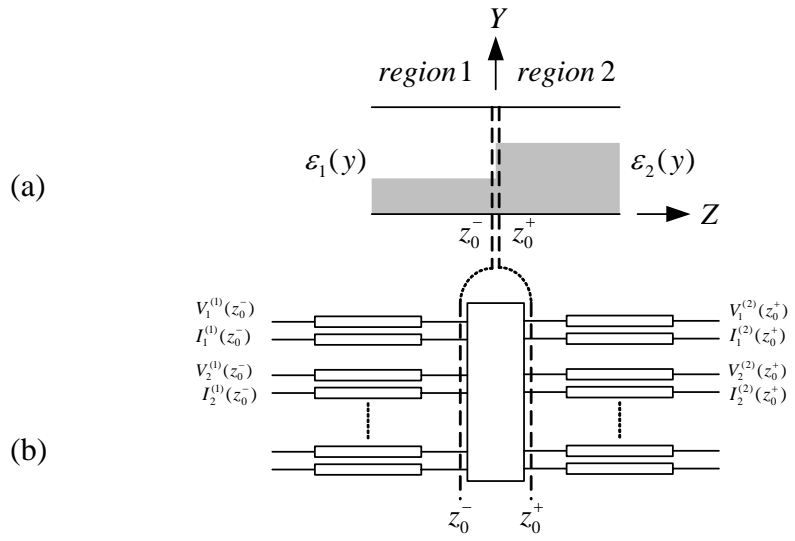

Fig 2.4   (a) A step discontinuity between two adjacent regions

(b) Equivalent network

9

could be expressed as the superposition of eigen modes in each region, which yields:

$$E_x^{(i)} = \sum_{n=1} \phi_n^{(i)}(y) V_n^{(i)}(z) \qquad\qquad (2\text{-}10)$$

$$H_y^{(i)} = \sum_{n=1} \phi_n^{(i)}(y) I_n^{(i)}(z) \qquad\qquad (2\text{-}11)$$

Where the amplitudes function in z direction, $V's$ and $I's$, characterized as voltage and current waves, satisfy the transmission-line equation along z direction as depicted in Fig 2.4 (b), written as:

$$\frac{dV_n^{(i)}(z)}{dz} = -jk_{z,n}^{(i)} Z_n^{(i)} I_n^{(i)}(z) \qquad\qquad (2\text{-}12)$$

$$\frac{dI_n^{(i)}(z)}{dz} = -jk_{z,n}^{(i)} Y_n^{(i)} V_n^{(i)}(z) \qquad\qquad (2\text{-}13)$$

Where $V_n^{(i)}(z)$ and $I_n^{(i)}(z)$ consist of both forward and backward propagating waves, $k_{z,n}^{(i)}$ is the propagating wavenumber defined in the section 2.2.1, $Z_n^{(i)} (= \frac{1}{Y_n^{(i)}})$ is the characteristic impedance (or admittance) along the z direction defined as below [10] (Appendix 1)

$$Z_n^{(i)} = \frac{\omega\mu_0}{k_{z,n}^{(i)}} \qquad \text{for TE mode} \qquad\qquad (2\text{-}14)$$

By imposing the boundary condition at the interface, the tangential electric and magnetic field components must be continuous at $z = z_0$ From (2-10) and (2-11), we have

$$\sum_{n=1}^{n_1} \phi_n^{(1)}(y) V_n^{(1)}(z_0^-) = \sum_{n=1}^{n_2} \phi_n^{(2)}(y) V_n^{(2)}(z_0^+) \qquad for\ E_x \qquad\qquad (2\text{-}15)$$

$$\sum_{n=1}^{n_1} \phi_n^{(1)}(y) I_n^{(1)}(z_0^-) = \sum_{n=1}^{n_2} \phi_n^{(2)}(y) I_n^{(2)}(z_0^+) \qquad for\ H_y \qquad\qquad (2\text{-}16)$$

Where $z_0^\pm = z_0 \pm \Delta z$, and Δz approaches to but not equal to zero, n_1 and n_2 denote the number of the modes employed in region1 and region2, respectively By multiplying

equations (2-15) and (2-16) with $\phi_m^{(1)}(y)$ at the both sides and taking the overlap integral for

the variable y from zero to h, we have

$$\sum_{n=1}^{n_1} V_n^{(1)}(z_0^-)\left\langle\phi_m^{(1)}(y)\big|\phi_n^{(1)}(y)\right\rangle = \sum_{n=1}^{n_2} V_n^{(2)}(z_0^+)\left\langle\phi_m^{(1)}(y)\big|\phi_n^{(2)}(y)\right\rangle \tag{2-17}$$

$$\sum_{n=1}^{n_1} I_n^{(1)}(z_0^-)\left\langle\phi_m^{(1)}(y)\big|\phi_n^{(1)}(y)\right\rangle = \sum_{n=1}^{n_2} I_n^{(2)}(z_0^+)\left\langle\phi_m^{(1)}(y)\big|\phi_n^{(2)}(y)\right\rangle \tag{2-18}$$

By invoking the orthogonal relation for the eigen mode, the above equations can be written

as:

$$V_m^{(1)}(z_0^-) = \sum_{n=1}^{n_2} V_n^{(2)}(z_0^+)\gamma_{mn} \tag{2-19}$$

$$I_m^{(1)}(z_0^-) = \sum_{n=1}^{n_2} I_n^{(2)}(z_0^+)\gamma_{mn} \tag{2-20}$$

$$\gamma_{mn} = \left\langle\phi_m^{(1)}(y)\big|\phi_n^{(2)}(y)\right\rangle \tag{2-21}$$

Where m ranges from one to n_1, n runs from one to n_2, γ_{mn} represents the coupling

between m^{th} and n^{th} mode in respective region   The above linear system of homogeneous

equations can be rewritten in the vector-matrix form, given below:

$$\underline{V_1} = \Re\underline{V_2} \tag{2-22}$$

$$\underline{I_1} = \Re\underline{I_2} \tag{2-23}$$

Where $\Re$ is defined as coupling matrix with its element γ_{mn} , $V's$ and $I's$ are the

voltage and current vectors with their mode amplitude filling in the entries   By multiplying

equations (2-15) and (2-16) with $\phi_m^{(2)}(y)$ at both sides and taking the overlap integral

incorporated with the orthogonal relation, we obtain the similar matrix equations given below:

$$\underline{V_2} = \Re^T\underline{V_1} \tag{2-24}$$

$$\underline{I_2} = \Re^T \underline{I_1} \tag{2-25}$$

Where the superscript T denotes the transpose of the coupling matrix $\Re$

After obtaining the coupling matrix between any two adjacent regions, we could further check the accuracy of these matrices [3] If the coupling matrix is not accurate, the condition of power conservation will not be present and some errors will occur Substituting (2-24) into (2-22) or (2-25) into (2-23), we have the unitary condition:

$$\Re\Re^T = I \tag{2-26}$$

Where I is the identity matrix In general, (2-26) may be considered as an criterion to see whether the coupling matrices are accurate or not in the numerical computation

2.2.3 Input-output relation

From the previous section, we have obtained the coupling matrix between two adjacent regions, each of which contains multiple uniform layers In this section, we will introduce a procedure to deal with the wave propagation through multiple discontinuities by using the input-output relation at the discontinuity and wave transition in a uniform waveguide Once the relationship described previously is obtained, we have a good position in figuring out the field components everywhere in the structure

Fig 2.5 (a) shows a parallel-plate waveguide filled with nonhomogeneous dielectric medium Since the dielectric medium is piecewise constant, we could partition them into three regions, which are denoted by $i-1$, i and $i+1$, respectively Besides, there are two

interfaces characterizing the discontinuities of the structure, which are $z = z_{i-1}$ and $z = z_i$, respectively Based on the mode matching method described in the previous section , the transmission-line network in the uniform waveguide and the transformer bank at the discontinuities could be drawn as depicted in Fig 2.5(b)
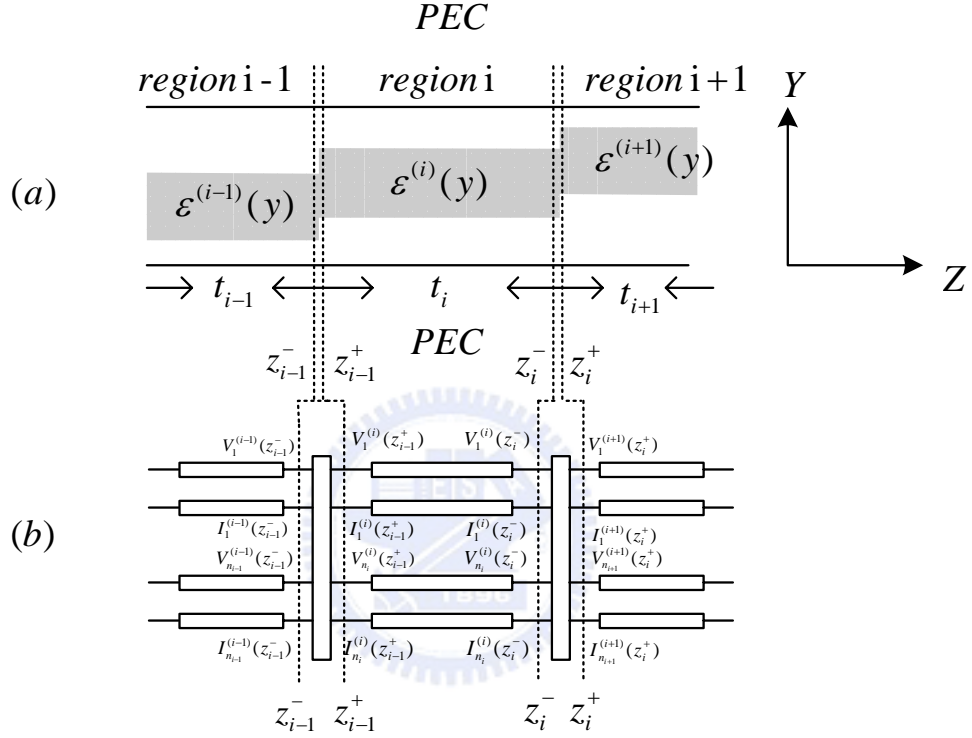

Fig 2.5   Equivalent network for a staircase structure

(a) Three regions

(b) Equivalent network

Here, we assume that the structure infinitely extends at the right hand side of Fig 2.5 (a), or the input impedance of each mode in the $i+1^{th}$ region is known   Thus, the input impedance matrix contains each mode in that region is assumed to be $Z_{in}^+(z_i^+)$ Where $Z_{in}^+(z_i^+)$ is a full matrix, which may include the mutual coupling effect due to waveguide modes in the present of discontinuities

After the input impedance matrix in the $i+1^{th}$ region at $z = z_i^+$ was given, we could

further transfer it from the right hand side of the interface, $z = z_i^+$ to the left one   Since the voltage and current waves in the region i and $i+1$ satisfy the relationship given in equation (2-22)~(2-25), we could obtain the input impedance matrix looking seen into the $i+1^{th}$ region at $z = z_i^-$, which is given below:

$$Z_{in}^- = \Re Z_{in}^+ \Re^T \tag{2-27}$$

In the previous section, we have transformed the input impedance matrix from the output region to the input region through a discontinuity by using the input-output relation of that discontinuity   Thus, in the next step, we should tackle the problem of wave transition in a uniform waveguide (in the ith region)   There are two problems to be handled, which are the input impedance matrix looking seen into the interface at $z = z_{i-1}^+$ and the transform matrix for the electric and magnetic fields from the output to the input interfaces of the finite section of waveguide (i^{th} region)

In a uniform waveguide, the voltage and current waves for each mode could be grouped into the vectors, which are given below:

$$\underline{V}(z) = \left\{V_n\,(z)\right\}_{n=1\ldots N} \tag{2-28}$$

$$\underline{I}(z) = \left\{I_n\,(z)\right\}_{n=1\ldots N} \tag{2-29}$$

For a finite length of transmission line, the voltage and current waves contain those of forward and backward propagation ones, which could be written as:

$$\underline{V}(z) = e^{-j\underline{\kappa}z}\,\underline{a} + e^{j\underline{\kappa}z}\,\underline{b} \tag{2-30}$$

$$\underline{I}(z) = Y\left[e^{-j\underline{\kappa}z}\,\underline{a} - e^{j\underline{\kappa}z}\,\underline{b}\right] \tag{2-31}$$

Where the matrix $e^{-j\underline{\kappa}z}$ is a diagonal matrix with its diagonal element representing the propagating constant along z direction for each mode, $\underline{a}$ and $\underline{b}$ are the amplitude vectors

consisting of each forward and backward propagating modes Besides, Y is the admittance matrix, each element representing the characteristic admittance of mode in the transmission line

Once the impedance matrix at the output of the transmission line is determined, we could further obtain the relationship between the forward and backward propagating amplitudes vectors $\underline{a}$ and $\underline{b}$ both at $z = z_i^-$ and $z = z_{i-1}^+$, which is given below:

$$\Gamma_{out} = (Z_{in}^- Y_i + I)^{-1}(Z_{in}^- Y_i - I) \tag{2-32}$$

$$\Gamma = e^{-j\underline{\kappa}t_i} \Gamma_{out} e^{-j\underline{\kappa}t_i} \tag{2-33}$$

Where Γ_{out} and Γ represent the reflection matrices at $z = z_i^-$ and $z = z_{i-1}^+$ Then, the input impedance matrix looking to the right at $z = z_{i-1}^+$ is determined by the impedance transform technique as:

$$Z_{in}^+ = (I + \Gamma)(I - \Gamma)^{-1}Z_i \tag{2-34}$$

From the mention above, the input-output relation for waves at the discontinuities and in each uniform waveguide are determined, we could sufficiently employ the equations (2-27),(2-32)~(2-34) to calculate the input impedance matrix from the last region to the first region Besides, the electric field components in each section could also be obtained by using the transfer matrices In detail speaking, if the input impedance matrix at the input interface is given as Z_{in} , thus we have the relationship between the forward and backward waves, which are written as :

$$\underline{b} = \Gamma_{in} \underline{a} \tag{2-35}$$

$$\Gamma_{in} = (Z_{in}Y_1 + I)^{-1}(Z_{in}Y_1 - I) \tag{2-36}$$

Where the Γ_{in} represents the reflection matrix at the input surface, $\underline{a}$ and $\underline{b}$ are those containing amplitudes of each waveguide mode Once the incident waveguide mode, $\underline{a}$, are

determined, the reflected amplitudes for each mode shall be totally understood in equation (2-35)   Thus, the voltage at the input surface could be given below:

$$\underline{V}(0) = (I + \Gamma_{in})\underline{a} \qquad (2\text{-}37)$$

Moreover, the voltage vector at the output surface could be obtained by the transfer matrix of each finite section and we assume that there are N basic units, which yields:

$$\underline{V}(\ell) = \left[\prod_{i=1}^{N} \mathrm{T}_i(t_i) \right] \underline{V}(0) \qquad (2\text{-}38)$$

Where $\underline{V}(\ell)$ is the voltage vector at the output surface ($z = \ell$), T_i is the transfer matrix consists of a step discontinuity and a uniform waveguide of thickness t_i Moreover, the input-output relation in a uniform waveguide is given below (Appendix 2):

$$\underline{V}(z_i^-) = (I + \Gamma_{out})e^{-j\kappa_i t_i}(I + \Gamma)^{-1}\underline{V}(z_{i-1}^+) \qquad (2\text{-}39)$$

In a word, by using the input-output relations for the discontinuity and uniform transmission line, we could simply figure out the electric field everywhere   Thus, the scattering characteristics of waveguide mode by an arbitrary nonhomogeneous structure could be understood by the procedures given in the previous paragraph

After determining the voltage and the current vectors in the input and output regions, we must check the principle of power conservation   This is the criterion to see whether the voltage and the current matrices are accurate or not   If the power is not conserved, the solution to this problem is not accurate By using the Poynting theorem, the formulation of the power conservation is shown as below:

$$\sum_{n=1}^{n_1} \mathrm{Re}\left[\left|V_{n,in}^{(1)}\right|^2 Y_0^{*(1)}\right] - \sum_{n=1}^{n_1} \mathrm{Re}\left[\left|V_{n,r}^{(1)}\right|^2 Y_0^{*(1)}\right] = \sum_{n=1}^{n_M} \mathrm{Re}\left[\left|V_{n,t}^{(M)}\right|^2 Y_0^{*(M)}\right] \qquad (2\text{-}40)$$

From the equation above, we can observe that the incident real power is equal to the sum of reflected and transmitted powers   In a word, the two factors affecting the power conservation are: (1) the eigen function in the transverse direction should form a complete set, and (2) the dispersion roots should be figured out rigorously   Fig 2.6 depicts the power conservation check versus a range of the wavelength for a specific structure   As shown in the figure, the power conservation is very good for a wide frequency band

After the power conservation is checked successfully, the next step is to check whether the tangential electric and the magnetic fields are continuous at the discontinuity   We have plotted the tangential electric and magnetic components in the respective region at the interface   Fig 2.7 (a) is the structural configuration and parameters of a junction discontinuity, wherein the two dielectric stabs have different thickness, however, they are infinitely extending   Fig 2.7 (b) and (c) depict the tangential electric and magnetic field components, respectively   The two figures exhibit the good agreement in the field continuity and prove the accuracy of the computational method in this thesis

(a)

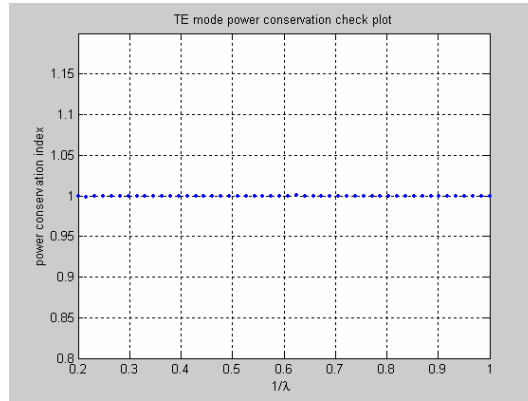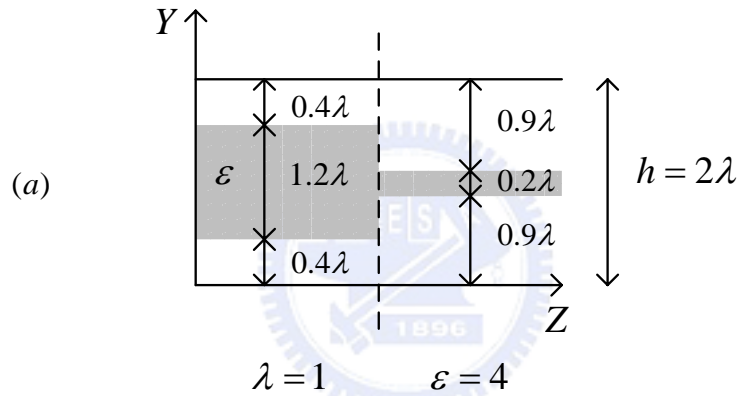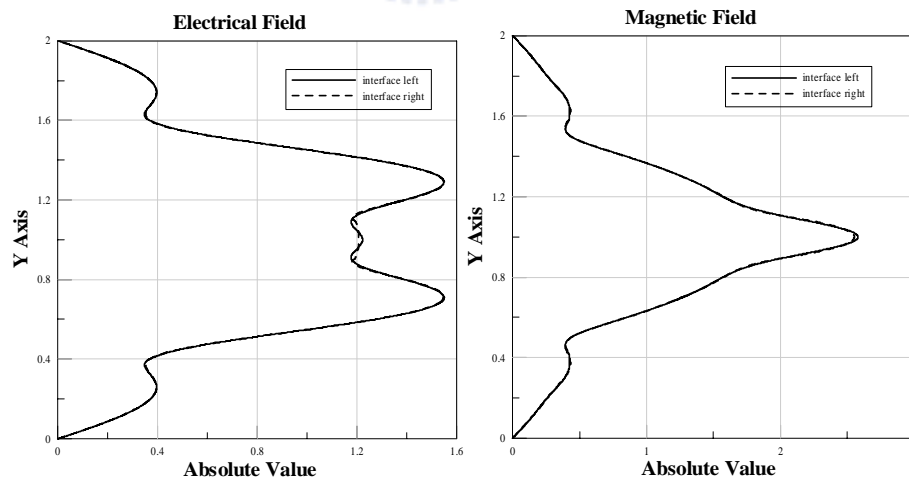$\lambda : 5 \sim 1 \qquad \varepsilon = 4$
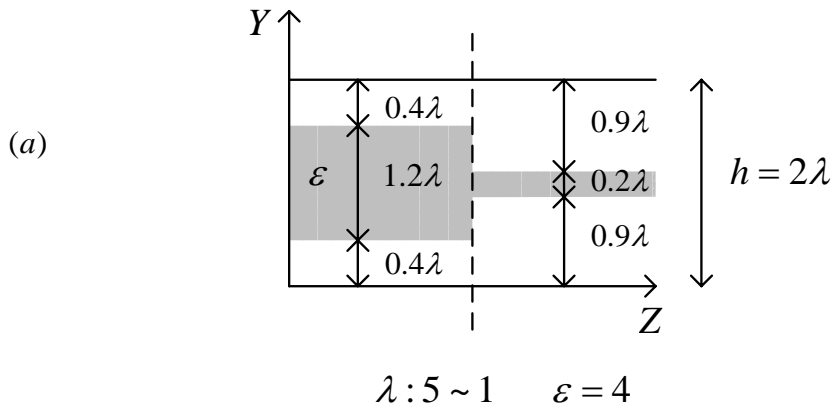
Fig 2.6　Power conservation check of one specific structure for TE mode

(a) A specific structure consists of two regions

(b) The power conservation check versus $1/\lambda$

Fig 2.7 Tangential E and H fields on the both sides of the interface for TE mode

(a) A specific structure consists of two regions

(b) The absolute value of the tangential electrical fields on the both sides at the junction discontinuity

(c) The absolute value of the tangential magnetic fields on the both sides at the junction discontinuity

18

Chapter 3

Numerical Results and Discussions

In this chapter, we will illustrate several typical transition structures which are often used in the optical circuits design   As is found in these figures, we plot the normalized power transmission versus a certain range of the transition length, and thus we can realize how long the transition length will be with the desired efficiency   Moreover, the power conservation is between 0.99990 and 1.00009 for most of the computing points   Finally, we will interpret the phenomenon existing in these figures with physical concepts, such that we can make sure the results we obtained are reasonable and acceptable

From Fig 3.2, we can easily observe that the results for these two cases will converge while $h > 7t_{thick}$, where t_{thick} is the thickness of the most thickest region in the structure Therefore, in the following analysis, we separate the distance of the parallel-plate waveguide larger than $8t_{thick}$ to approximate the practical situation   Furthermore, for a certain T, we also test how many steps or basic units are needed to approximate the continuous profile of the transition structure   As is found in Fig 3.3, the number of the steps for a certain T is at least $4 \times \dfrac{T}{\lambda}$ to receive the convergent result

Consider the first case of transition for a step discontinuity between two uniform

waveguides with different thickness as shown in Fig 3.4 The first surface wave mode (TE_1) is fed from thick waveguide into thin one which is placed on the bottom of the structure Moreover, there is only one surface wave mode existing in the thin waveguide Here, we illustrate six different value of t_1 and Δh represents the distance between t_1 and t_2 We observe that as Δh is greater, a longer transition length (T) is needed to transmit over 95% incident power successfully, such as $T > 0.75\lambda$ for $t_1 = 0.4\lambda$ and $T > 3.5\lambda$ for $t_1 = 0.8\lambda$ The interpretation is that as Δh is increasing, for a fixed number of steps (N_c), the variation of the characteristic impedance (ΔZ) along the z direction between adjacent regions is increasing as well, thus we will have a worse transmission at the discontinuity as shown in Fig 3.1 Where Z and k denote the characteristic impedance and the wavenumber along the z direction , $\dfrac{T}{N_c}$ represents the length of one region (step)
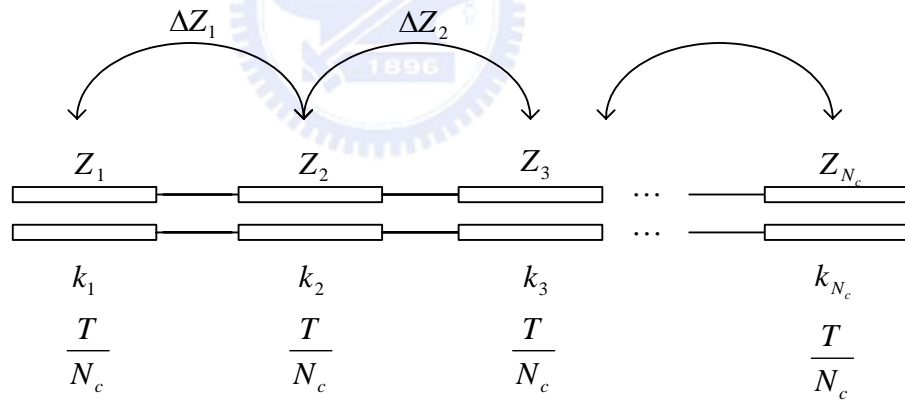

Fig 3.1 The equivalent network of the transition structure

Fig 3.5 shows the same condition with Fig 3.4 for greater Δh for all cases With the same interpretation above, as is expected, the transmission is worse than in Fig 3.4 and a longer T is needed to receive the same desired transmission efficiency

Fig 3.6 depicts the condition that the thin waveguide is placed in the central of the

structure　For all cases, we can observe that the transmission is better than previous figure

The interpretation is that, as the thin waveguide is closer to the central of the structure, ΔZ is smaller between adjacent regions, such that the transmission is better at the discontinuity

Fig 3.7 depicts another case of transition for a step discontinuity between two uniform waveguides　Compared with Fig 3.4, we can observe that the transmission in Fig 3.7 is much better while TE_1 is fed from thin waveguide into thick one　The interpretation is that there are more than one surface wave mode existing in the thick waveguide, and thus the magnitude of coupling is much stronger at the discontinuity　Fig 3.8 depicts the same condition with Fig 3.7 for a smaller t_1　As is expected, with larger Δh for all cases, the transmission is worse than in Fig 3.7 and the interpretation has been mentioned in the third paragraph

Fig 3.9 shows the transmission characteristics of bended waveguides with two different cases　The profile of the transition region is formulated by the following equation:

$$y = \tanh(\frac{x}{0.91024T}) \times a\lambda \qquad (4\text{-}1)$$

Where T represents the transition length, $a\lambda$ represents the distance between the two waveguides axes　Obviously observed from (a) and (b), the transmission is worse while the distance between the two waveguides axes is longer　Another phenomenon is that the transmission of the thick case is better than the thin one　The interpretation is that the number of the surface wave modes in the thick case is more than the thin one, thus the coupling is stronger at the discontinuity and a better transmission will be obtained

Fig 3.10 shows the transmission characteristics of another bended type waveguide with two different thickness　The number of the surface wave modes are one and two for $t = 0.1\lambda$

and $t = 0.35\lambda$, respectively The profile is symmetric and the left half of the transition region is formulated by the following equation:

$$y = \tanh(\frac{x}{T}) \times \lambda \qquad\qquad (4\text{-}2)$$

Where T and λ represent the transition length and the operating wavelength Observed from this figure, with the same interpretation mentioned in the previous paragraph, the transmission is better for the thick case than for the thin one

Fig 3.11 shows the transmission characteristics of the perturbed waveguide with three different cases From this figure, we can observe that as the lower bound of the transition region is more flat, the transmission is better

Fig 3.12 shows the transmission characteristics of a crack waveguide with three different cases From this figure, we can observe that , when $T = 0$, the transmission is worse while the length of S is longer, such as $P_t = 0.58$ for $S = 0.6\lambda$ and $P_t = 0.52$ for $S = 1.2\lambda$ As is found, the transition length is at least 3λ for over 95% power can be transmitted successfully for these three cases Fig 3.13 shows the same condition with Fig 3.12 for a deeper crack waveguide As is expected, the transmission is worse and the transition length is longer than Fig 3.12 for the same desired transmission efficiency An interesting phenomenon can also be observed from Fig 3.12 and Fig 3.13 that, while the transition length is greater than about 1.5λ, the curves in both figures will get very closely to each other The interpretation of such a phenomenon is listed as below First, we can divide the crack waveguide in Fig 3.12 into two half parts, the left half side is the same with the Fig 3.4, and the right half side is the same with the Fig 3.7 From Fig 3.7, we can easily observe

that, for $t_2 = 0.8\lambda$, over 99% power can be transmitted while the transition length is greater than 1.5λ Therefore, while $T > 1.5\lambda$, the curves in Fig 3.12 for all cases are dominated by Fig 3.4, such that these different cases can be seen as the similar ones
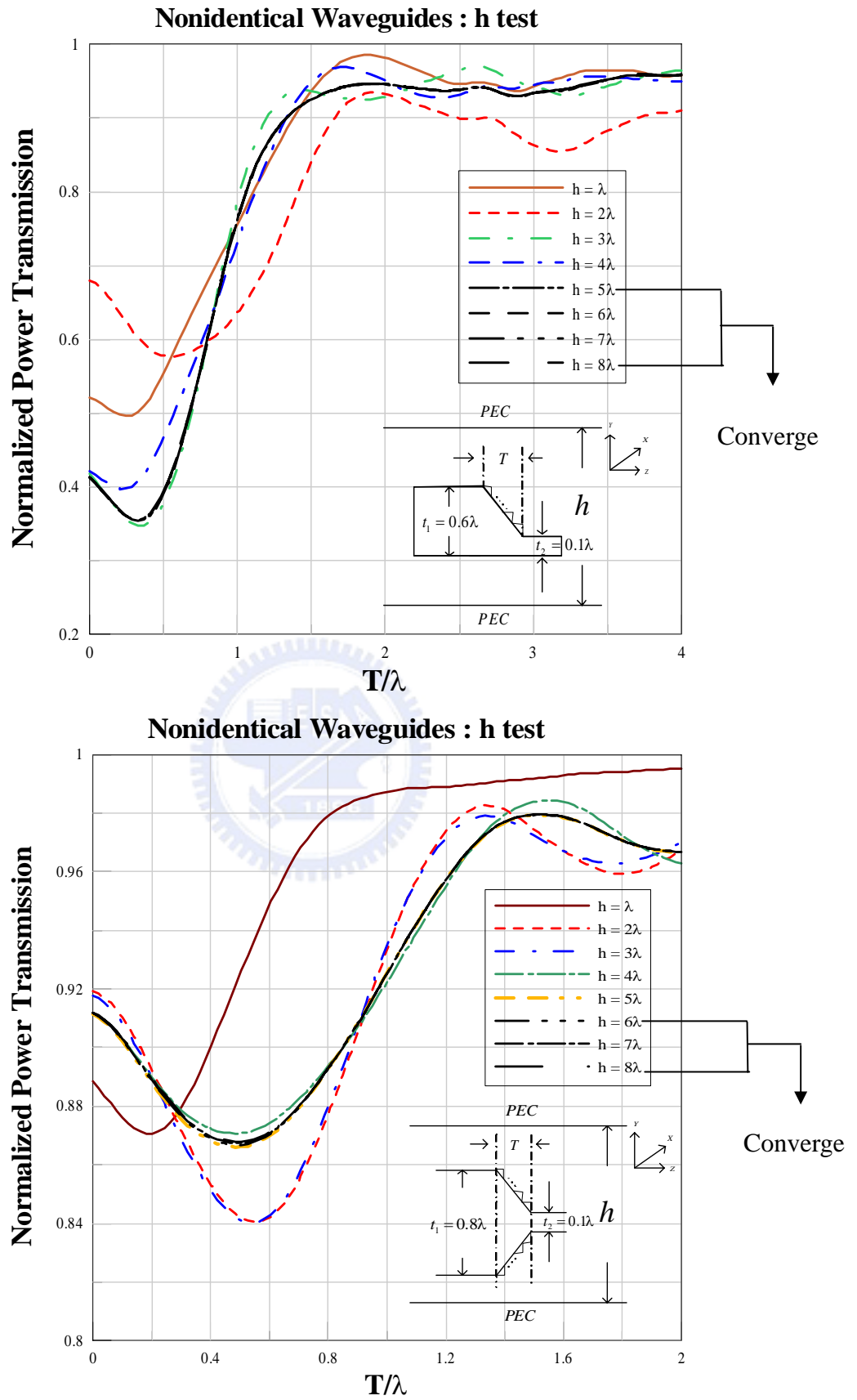
Fig 3.2 Test the separation distance of the parallel-plate waveguide to pursue the convergent result

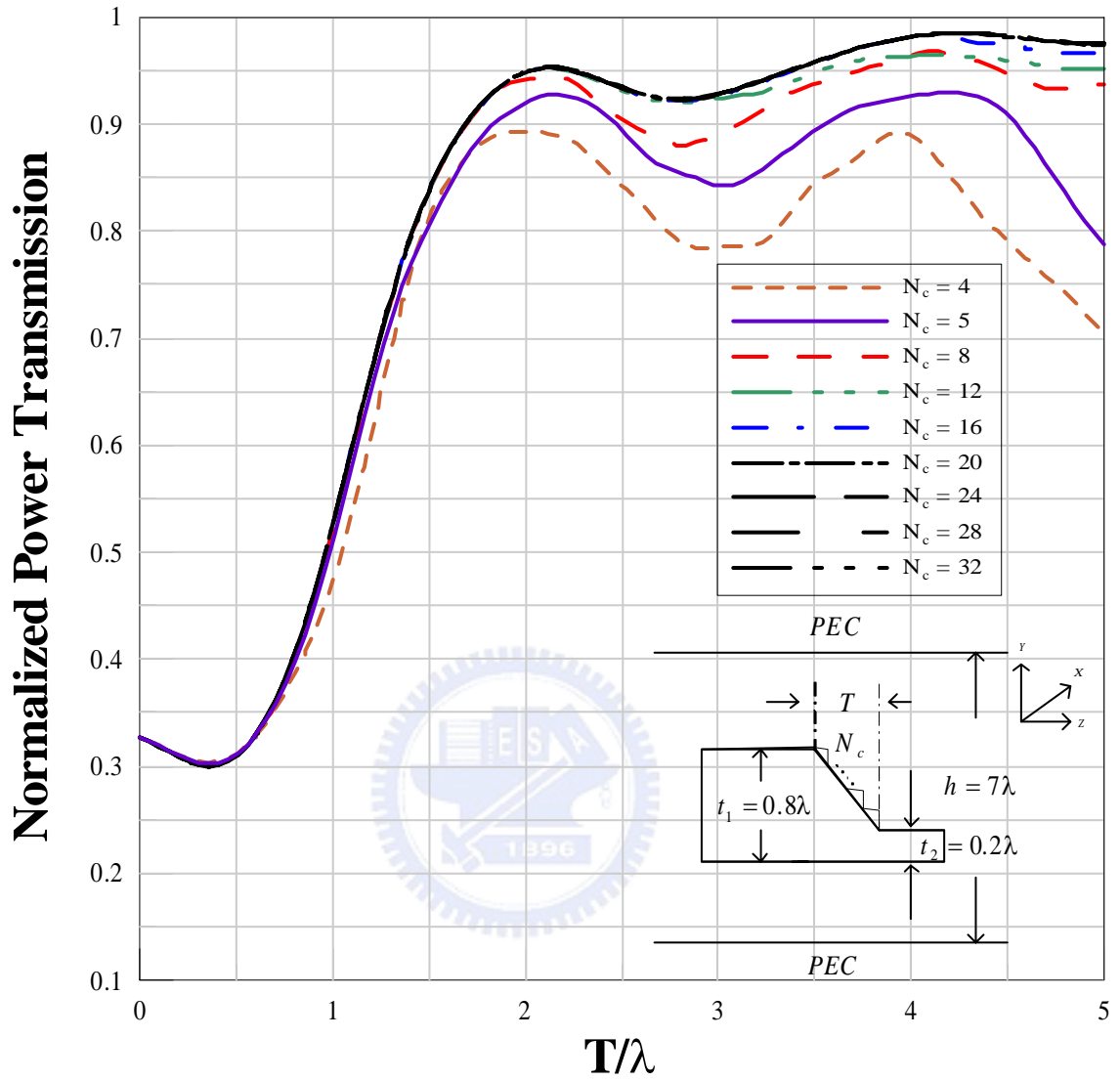# Nonidentical Waveguides : staircase test

Fig 3.3   Test N_c to pursue the convergent result

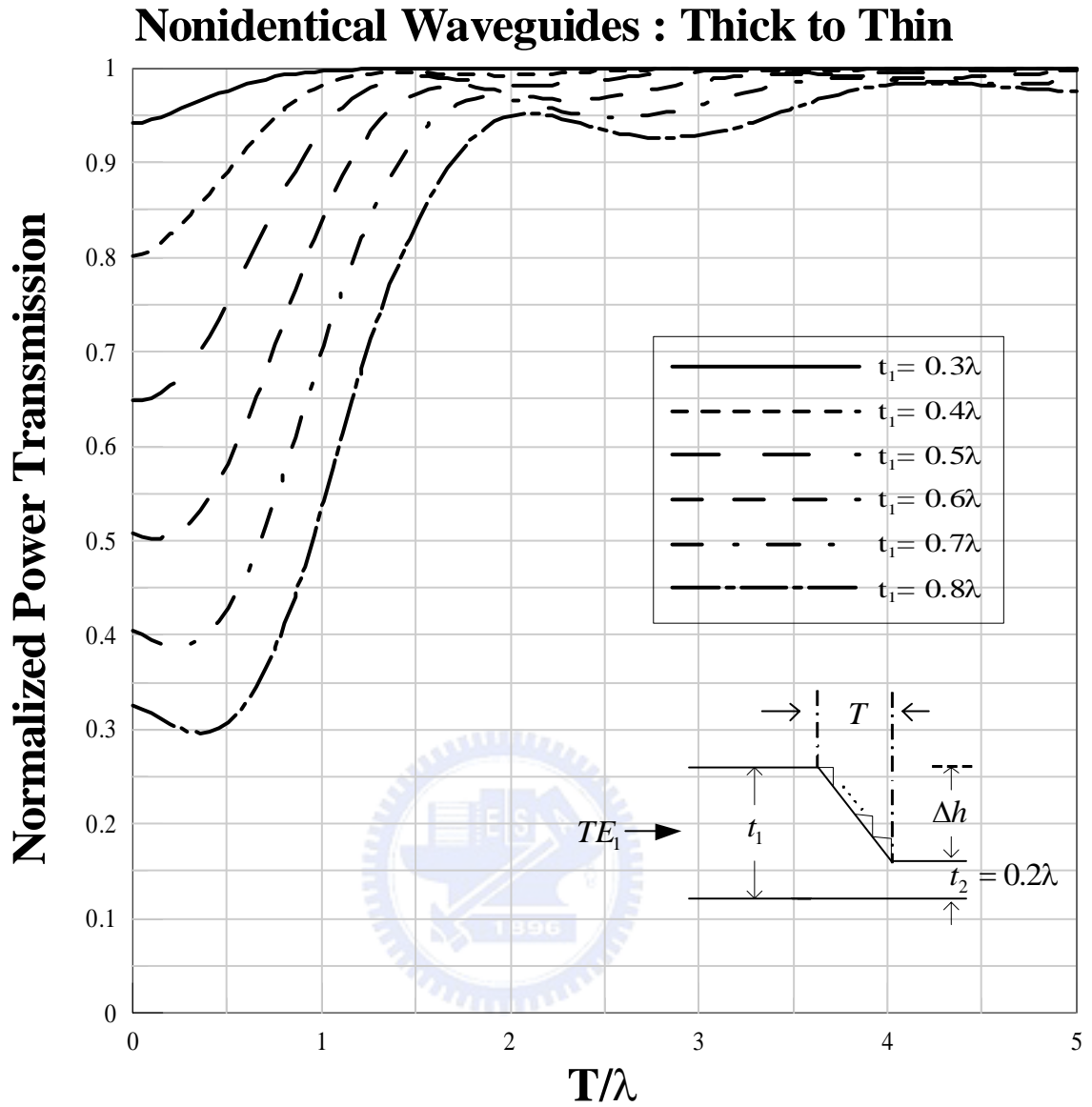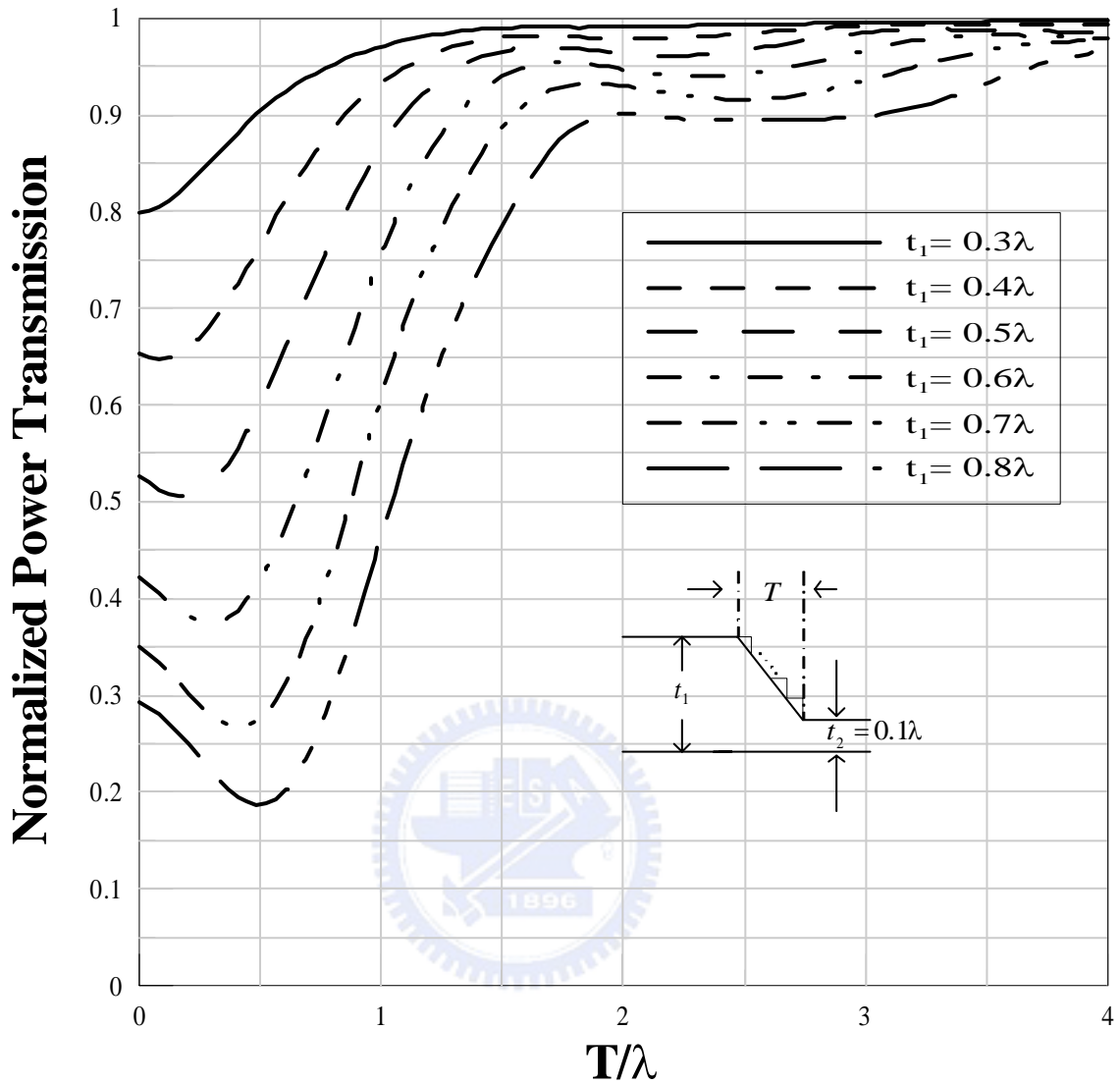# Nonidentical Waveguides : Thick to Thin

Fig 3.4   Transmission through two uniform waveguides with different thickness: Thick to Thin

The thin waveguide is placed on the bottom of the structure $t_2 = 0.2\lambda$

TE mode, $P_{in} = 1$, $\varepsilon = 4$

Fig 3.5 Transmission through two uniform waveguides with different thickness: Thick to Thin

The thin waveguide is placed on the bottom of the structure $t_2 = 0.1\lambda$
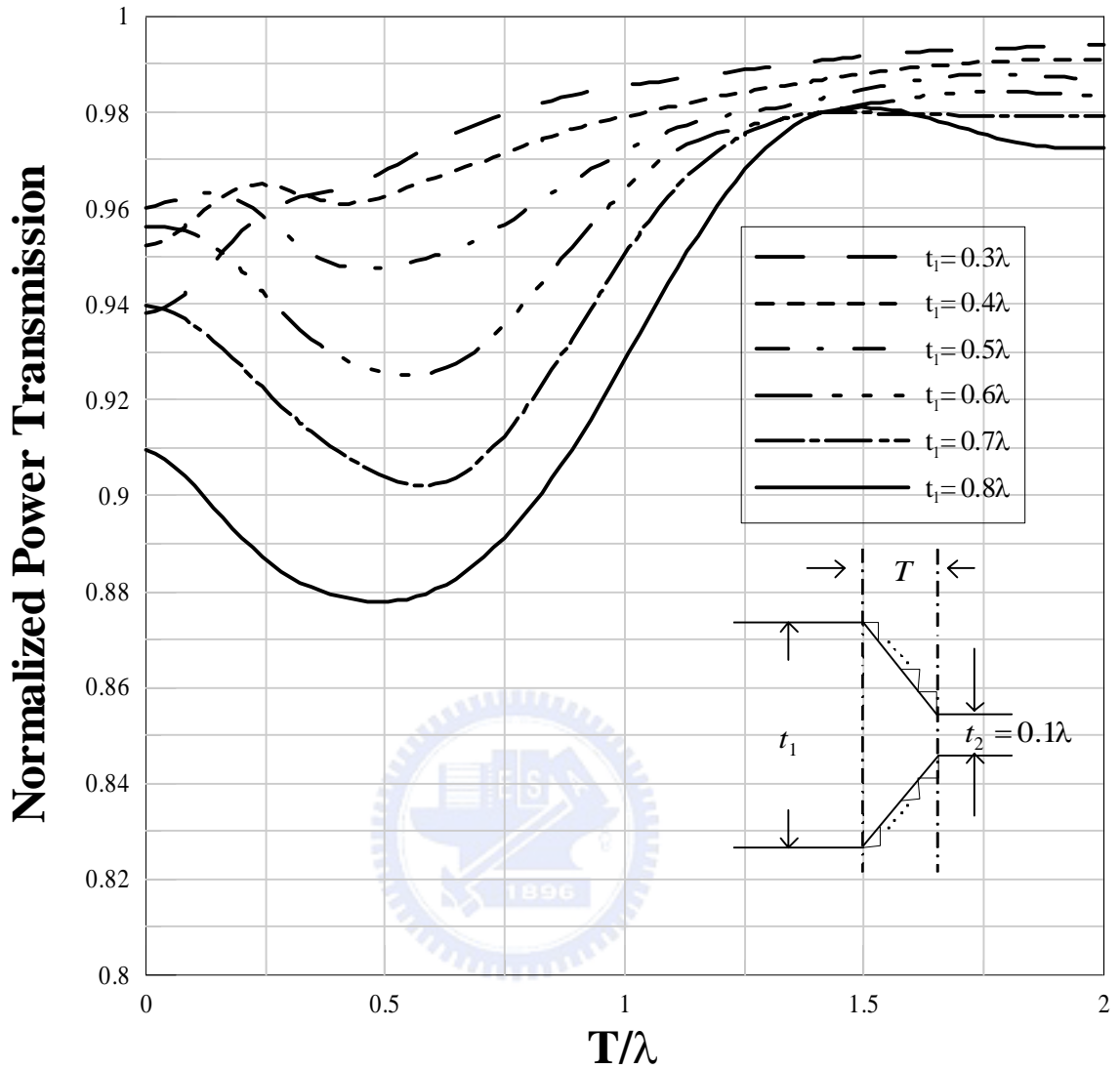
TE mode, $P_{in} = 1$, $\varepsilon = 4$

Fig 3.6   Transmission through two uniform waveguides with different thickness: Thick to Thin
The thin waveguide is placed in the central of the structure $t_2 = 0.1\lambda$
TE mode, $P_{in} = 1$, $\varepsilon = 4$
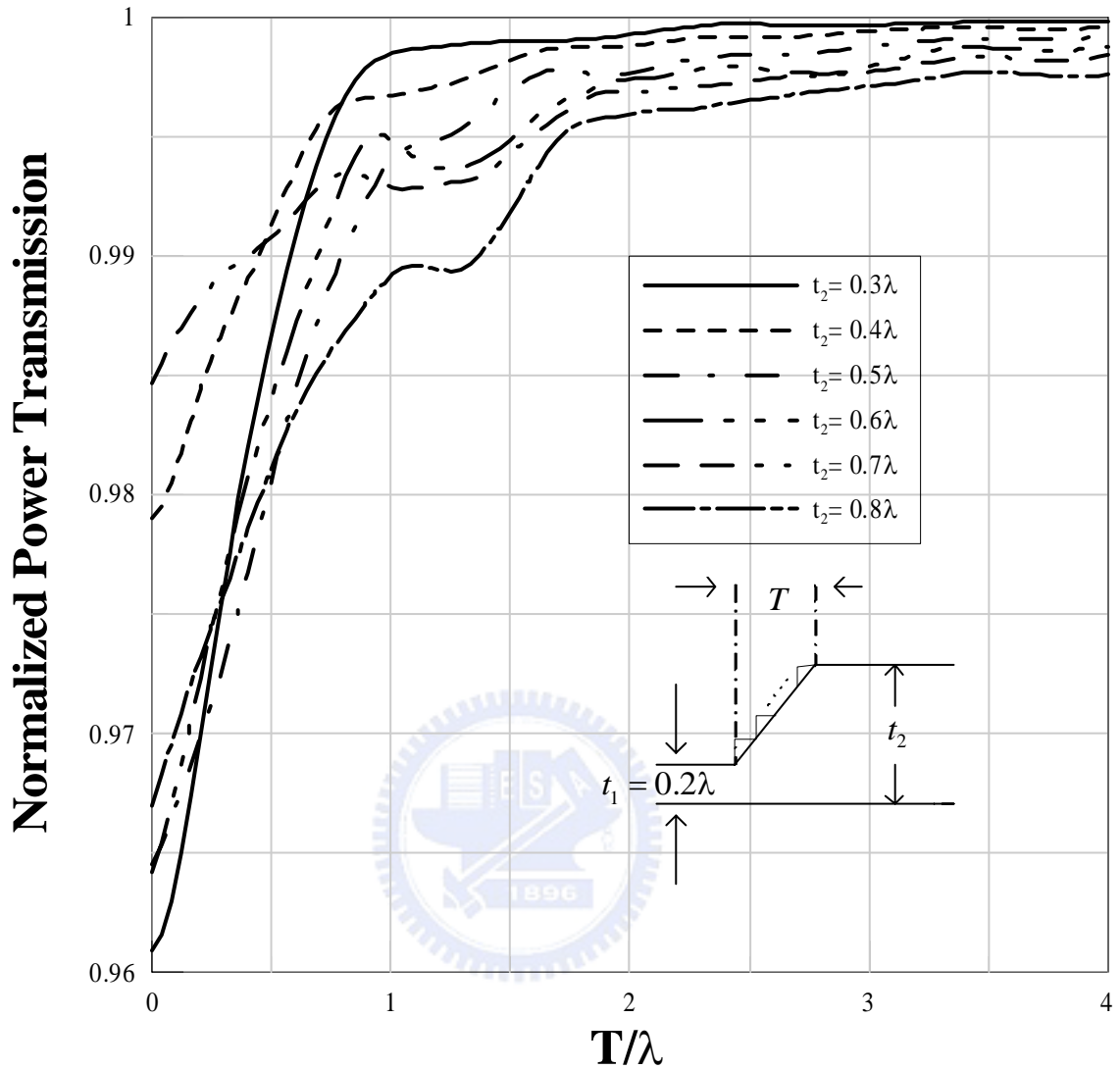
Nonidentical Waveguides : Thin to Thick

Fig 3.7   Transmission through two uniform waveguides with different thickness: Thin to Thick

The thin waveguide is placed on the bottom of the structure $t_1 = 0.2\lambda$

TE mode, $P_{in} = 1$, $\varepsilon = 4$
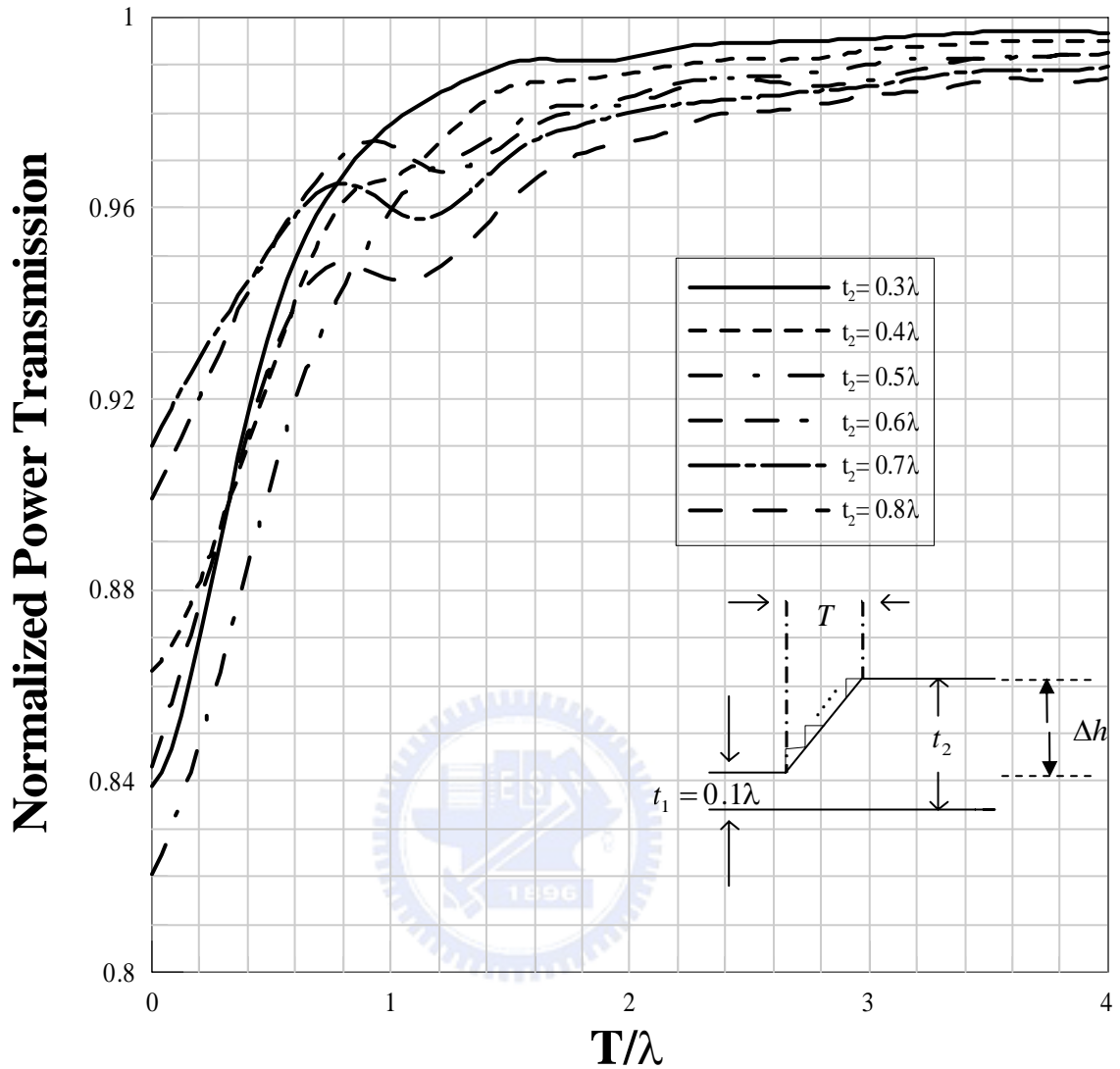
Nonidentical Waveguides : Thin to Thick

Fig 3.8   Transmission through two uniform waveguides with different thickness: Thin to Thick

The thin waveguide is placed on the bottom of the structure $t_1 = 0.1\lambda$

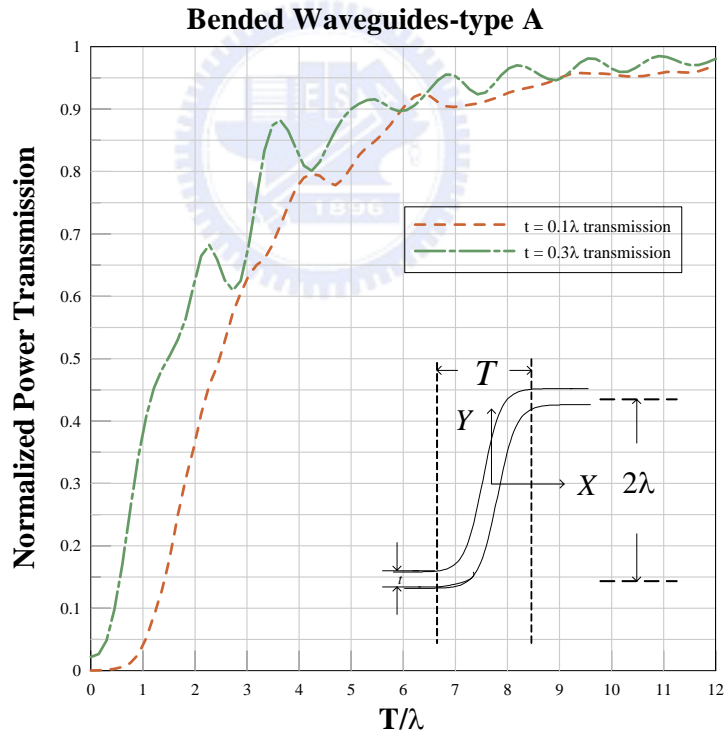TE mode, $P_{in} = 1$, $\varepsilon = 4$

Bended Waveguides-type A

Bended Waveguides-type A
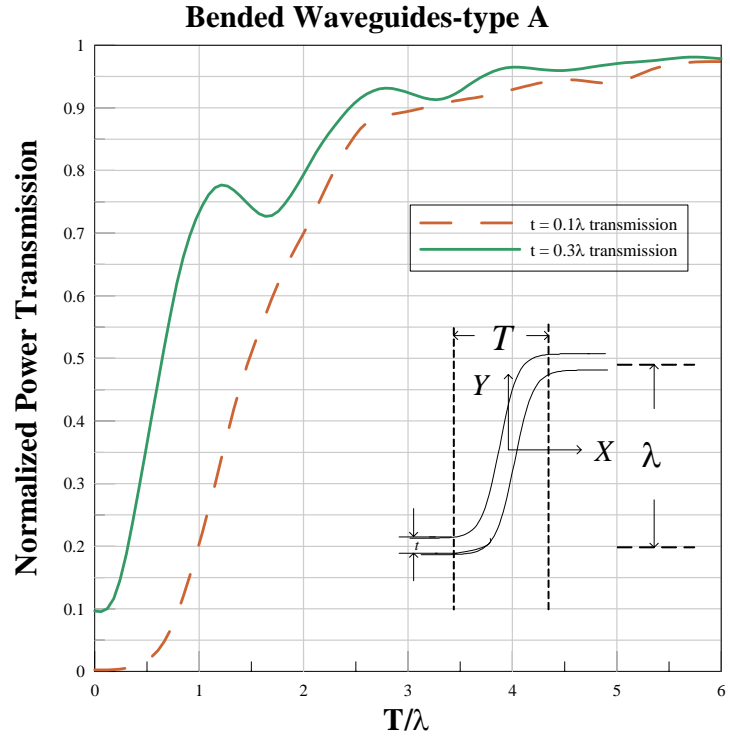

Fig 3.9   Transmission efficiencies of bended waveguides (type A)
with two different thickness

TE mode, $P_{in} = 1$, $\varepsilon = 4$, $y = \tanh(\dfrac{x}{0.91024T}) \times a\lambda$

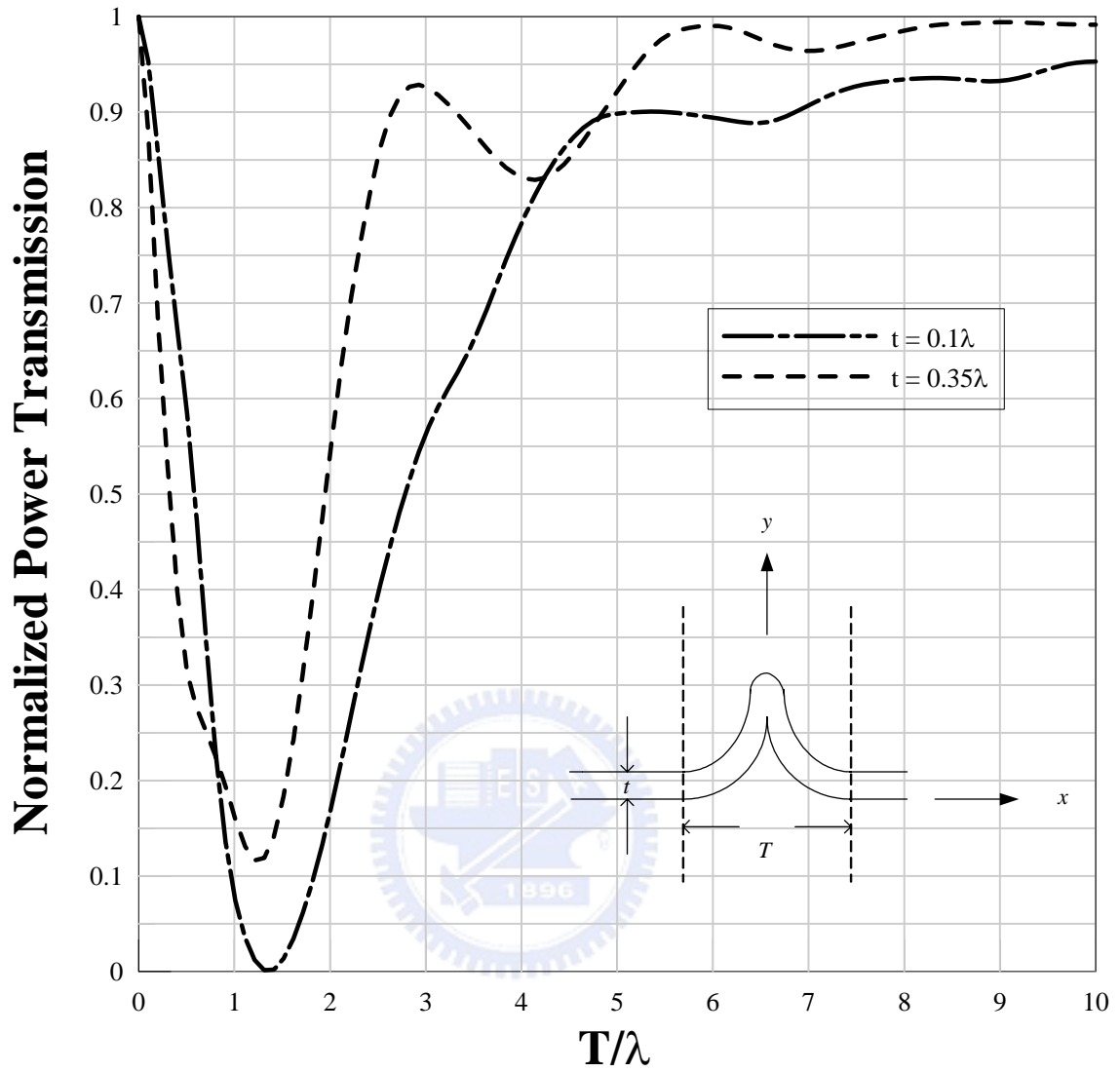(a) $a = 1$

(b) $a = 2$

Bended Waveguides-type B

Fig 3.10   Transmission efficiency of a bended waveguide (type B)
with two different thickness

TE mode, $P_{in} = 1$, $\varepsilon = 4$, $y = \tanh(\frac{x}{T}) \times \lambda$

Perturbed Waveguides
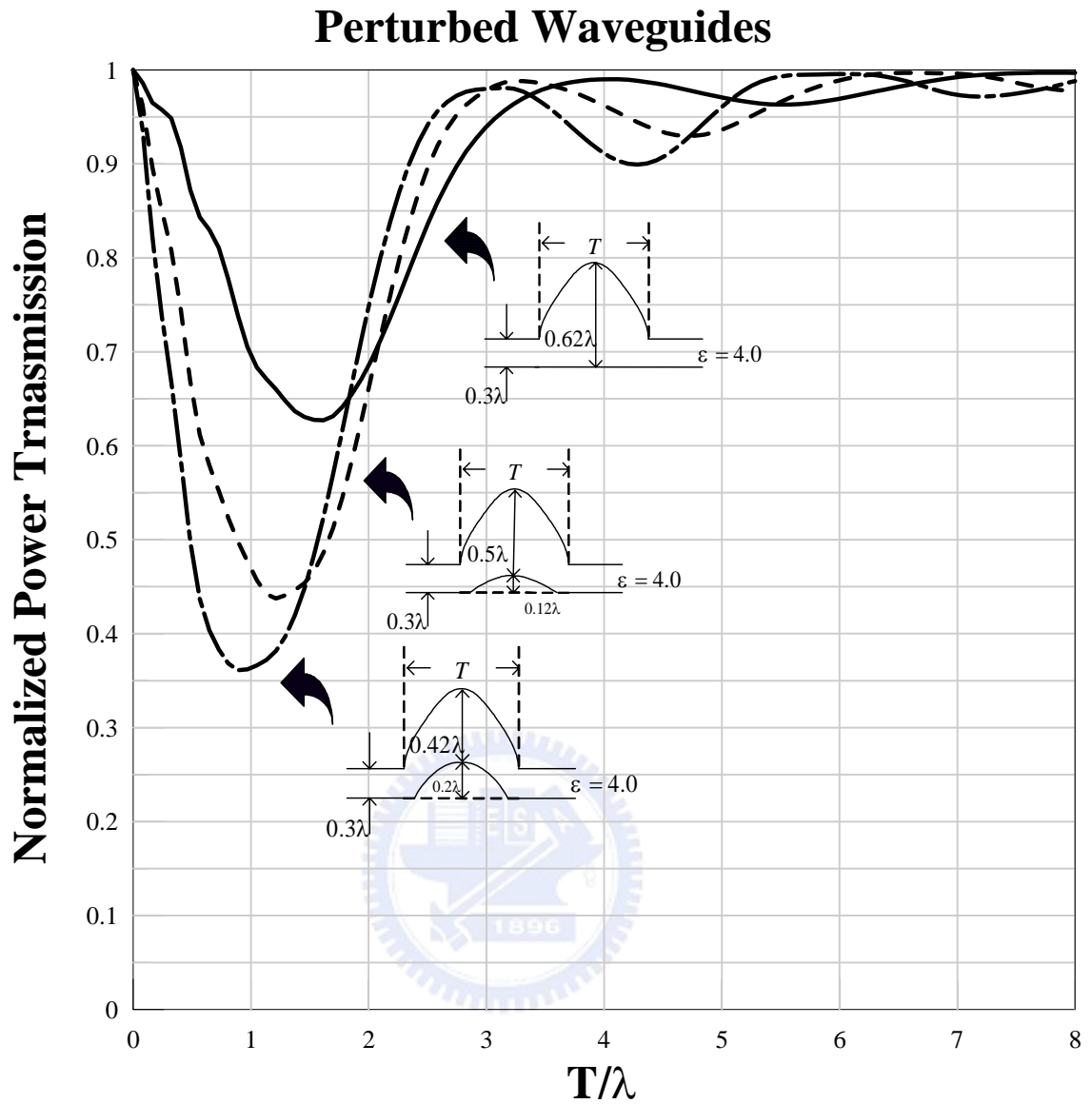
Fig 3.11   Comparison between three perturbed waveguides of different types

TE mode, $P_{in} = 1$, $\varepsilon = 4$
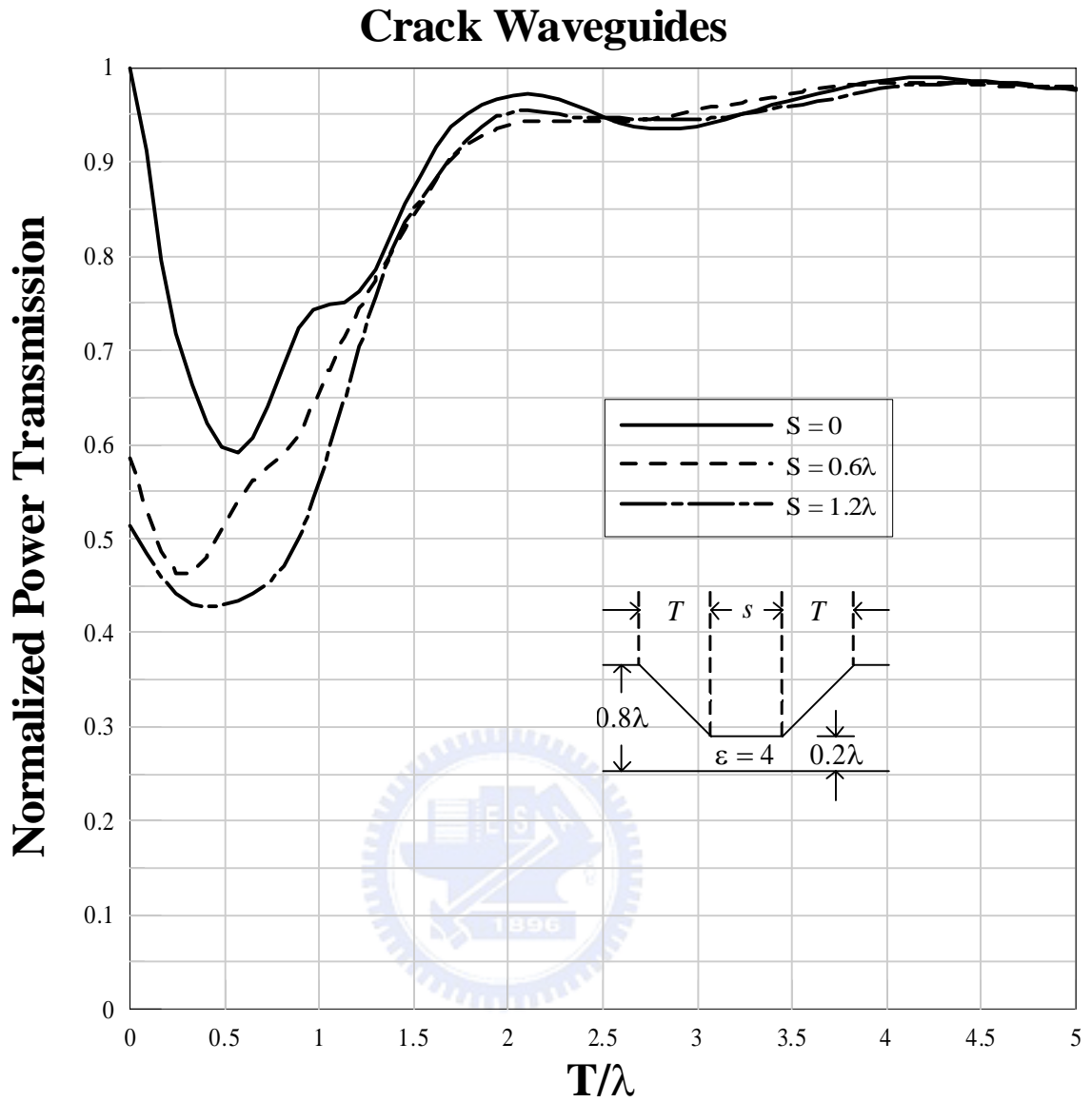
Crack Waveguides

Fig 3.12   Transmission through a crack with three different types

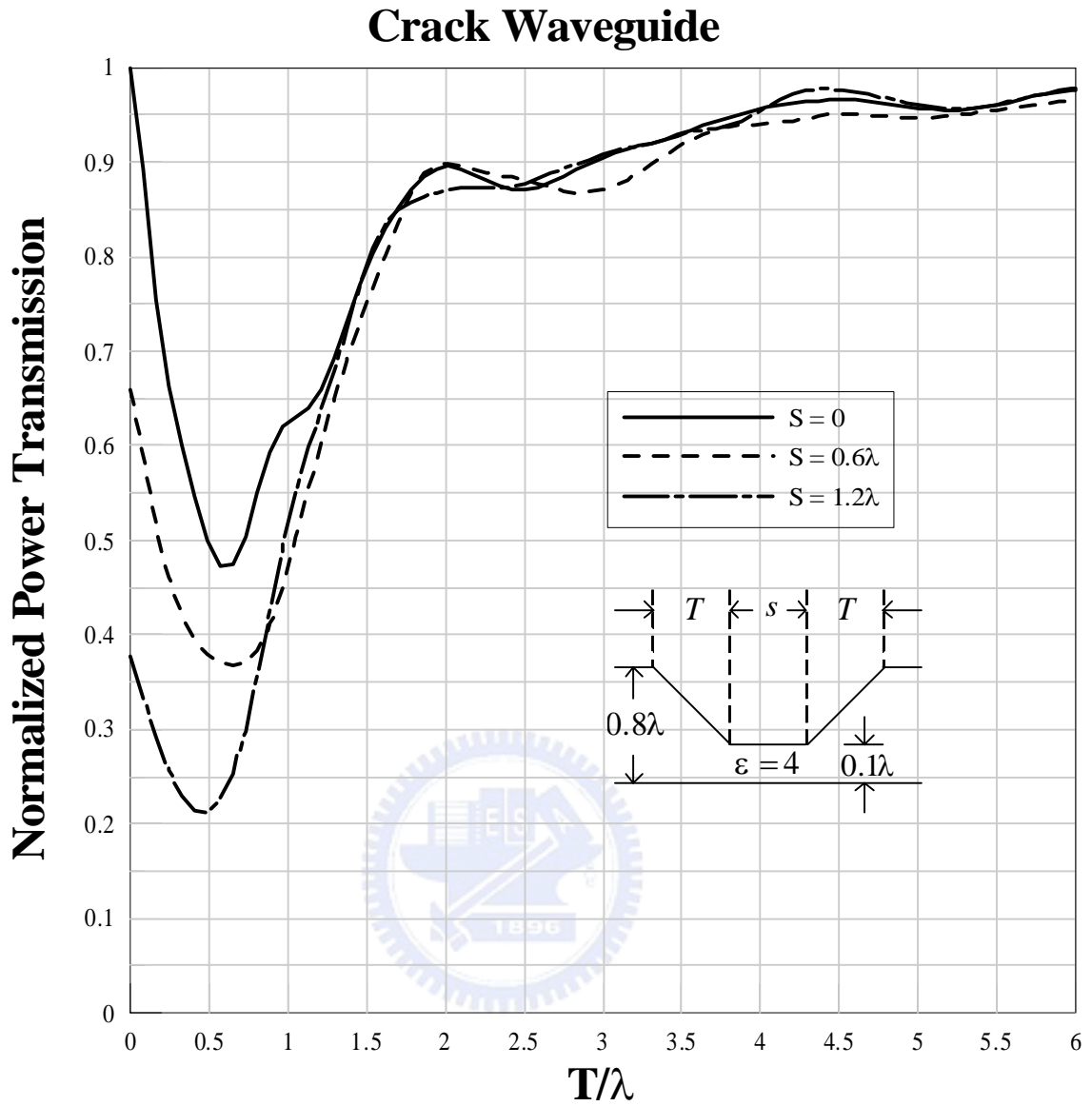TE mode, $P_{in} = 1$, $\varepsilon = 4$

Crack Waveguide

Fig 3.13   Transmission through a crack with three different types

A deeper case than Fig 3.12

TE mode, $P_{in} = 1$, $\varepsilon = 4$

Chapter 4

Conclusion

———————————

To sum up, we have formulated a systematic way to analyze any type of the transition structure by using the staircase approximation and the mode matching method In the process of the analysis, by separating the distance of the parallel-plate waveguide far enough and adopting sufficient number of steps, we can receive the corresponding results which are expected approaching the practical situation

From the previous chapter, we have surveyed a large class of transition structures while the first surface wave mode is incident form the left With the extensive numerical results, we can easily observe that we need a longer transition length to receive the desired transmission efficiency while the variation of the structure is getting greater Moreover, as the number of the surface wave modes in the dielectric waveguide is greater, the coupling is stronger at the discontinuity Above all, from these figures, we have developed a useful criterion to design the transition structures with the desired transmission efficiency

Appendix

Appendix 1: The characteristic impedance along the Z direction

for TE mode

From reference [10], we can receive the relationship between the transverse E and H fields as shown in below:

$$\kappa_i Z_i \underline{e}_i(x, y) = \omega\mu(\underline{\underline{1}}_t + \frac{\underline{\underline{\nabla}}_t}{k_0^2 \varepsilon(y)}) \cdot (\underline{h}_i(x, y) \times \underline{z}_0) \tag{1}$$

$$\kappa_i Y_i \underline{h}_i(x, y) = \omega\varepsilon_0\varepsilon(y)(\underline{\underline{1}}_t + \frac{\underline{\underline{\nabla}}_t}{k_0^2 \varepsilon(y)}) \cdot (\underline{z}_0 \times \underline{e}_i(x, y)) \tag{2}$$

Where i represents the ith mode, $\underline{e}_i(x, y)$ and $\underline{h}_i(x, y)$ represent the transverse distribution of the transverse electric and magnetic components   For TE mode, the transverse field components are listed as below:

$$E_{xi} = \phi_i(y)V_i(z) \tag{3}$$

$$H_{yi} = \phi_i(y)I_i(z) \tag{4}$$

$$H_{zi} = \frac{1}{-j\omega\mu_0}\frac{d\phi_i(y)}{dy}V_i(z) \tag{5}$$

Substituting (3)~(5) into (2), we can receive:

$$\kappa_i Y_i \phi_i(y)\underline{y}_0 = \omega\varepsilon_0\varepsilon(y)[(\underline{x}_0\underline{x}_0 + \underline{y}_0\underline{y}_0) + (\frac{\frac{\partial^2}{\partial x^2}\underline{x}_0 + \frac{\partial^2}{\partial x\partial y}\underline{y}_0}{k_0^2\varepsilon(y)}\underline{x}_0 + \frac{\frac{\partial^2}{\partial x\partial y}\underline{x}_0 + \frac{\partial^2}{\partial y^2}\underline{y}_0}{k_0^2\varepsilon(y)}\underline{y}_0)] \cdot$$

$$(\underline{z}_0 \times \phi_i(y)\underline{x}_0) \tag{6}$$

From the equation above, we have two relations:

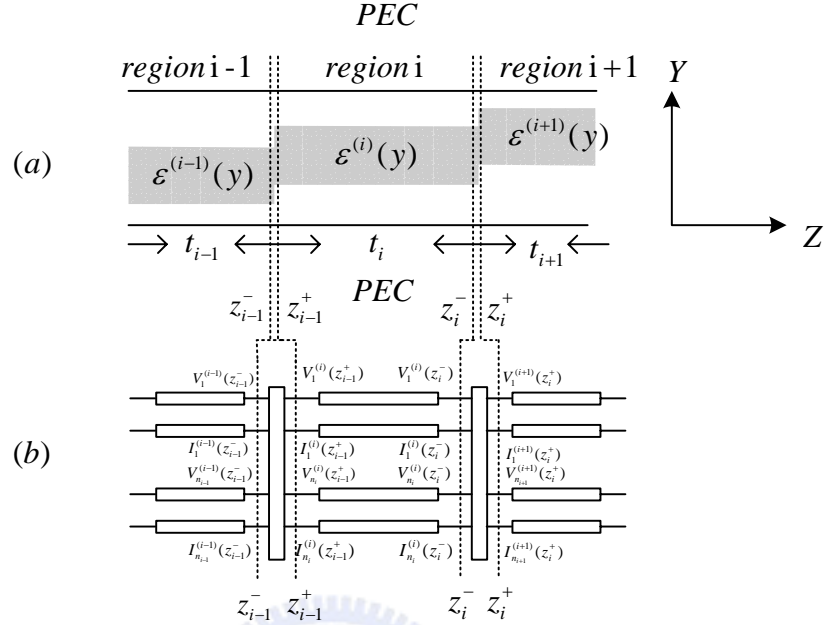1. $\kappa_i Z_i \phi_i(y)\underline{x_0} = \omega\mu\phi_i(y)\underline{x_0}$

2. $\kappa_i Y_i \phi_i(y)\underline{y_0} = \omega\varepsilon_0\varepsilon(y)[(\phi_i(y)\underline{y_0}) + (\dfrac{\dfrac{\partial^2\phi_i(y)}{\partial y^2}}{k_0^2\varepsilon(y)}\underline{y_0})]$

From relation 1, we can determine the characteristic impedance for TE mode along the z direction as below:

$$Z_i = \frac{\omega\mu}{\kappa_i} \tag{7}$$

Appendix 2: The input-output relation in the uniform waveguide

From this figure, we assume that we have received the voltage vector, $\underline{V}(z_{i-1}^+)$, at the $i-1^{th}$ interface, and then we must implement several steps to find the voltage vector at the next interface in the same region

First of all, the expressions of the forward amplitude vector, $\underline{a}$, at $z = z_{i-1}^+$ is given by:

$$\underline{a} = (I + \Gamma)^{-1} \underline{V}(z_{i-1}^+) \tag{1}$$

Where Γ is the reflection coefficient matrix at $z = z_{i-1}^+$, I is the unitary matrix   As we know, Γ can be expressed as follows:

$$\Gamma = e^{-j\underline{\kappa}t_i} \Gamma_{out} e^{-j\underline{\kappa}t_i} \tag{2}$$

Where Γ_{out} is the reflection coefficient matrix at $z = z_i^-$ Moreover, the voltage vector at $z = z_i^-$, $\underline{V}(z_i^-)$, can be expressed as follows:

$$\underline{V}(z_i^-) = e^{-j\underline{\kappa}t_i} \underline{a} + e^{j\underline{\kappa}t_i} \Gamma \underline{a} \tag{3}$$

Substitute (2) into (3), we have:

$$\underline{V}(z_i^-) = (I + \Gamma_{out})e^{-j\underline{\kappa}l_i}\,\underline{a} \tag{4}$$

Finally, we substitute (1) into (4), then we have:

$$\underline{V}(z_i^-) = (I + \Gamma_{out})e^{-j\underline{\kappa}l_i}(I + \Gamma)^{-1}\underline{V}(z_{i-1}^+) \tag{5}$$

From equation (5), we have successfully received $\underline{V}(z_i^-)$ by transferring $\underline{V}(z_{i-1}^+)$ and the

input-output relation in a uniform waveguide is defined as:

$$(I + \Gamma_{out})e^{-j\underline{\kappa}l_i}(I + \Gamma)^{-1} \tag{6}$$

Bibliography

[1] *Song-Tsuen Peng; Oliner, A.A.* **"Guidance and Leakage Properties of a Class of Open Dielectric Waveguides: Part I--Mathematical Formulations"** Microwave Theory and Techniques, IEEE Transactions on , Volume: 29 , Issue: 9 , Sep 1981 , Pages: 843 - 855

[2] *Oliner, A.A.; Song-Tsuen Peng; Ting-Ih Hsu; Sanchez, A.* **"Guidance and Leakage Properties of a Class of Open Dielectric Waveguides: Part II--New Physical Effects"** Microwave Theory and Techniques, IEEE Transactions on , Volume: 29 , Issue: 9 , Sep 1981 , Pages: 855 − 869

[3] *Ruey Bing Hwang* **"The improvement of tri-plate line performance by using corrugated transitions"** Electromagnetic Compatibility, IEEE Transactions on , Volume: 42 , Issue: 4 , Nov. 2000 , Pages: 314 - 325

[4] *Brooke, G.H.; Kharadly, M.M.Z* **"Scattering by Abrupt Discontinuities on Planar Dielectric Waveguides"** Microwave Theory and Techniques, IEEE Transactions on , Volume: 82 , Issue: 5 , May 1982 , Pages: 760 − 770

[5] *Shigesawa, H.; Tsuji, M.* **"Mode Propagation through a Step Discontinuity in Dielectric Planar Waveguide"** Microwave Theory and Techniques, IEEE Transactions on , Volume: 34 , Issue: 2 , Feb 1986 , Pages: 205 − 212

[6] *Lewin* **"Radiation from Curved Dielectric Slabs and Fibers"** Microwave Theory and Techniques, IEEE Transactions on , Volume: 22 , Issue: 7 , Jul 1974 , Pages: 718 − 727

[7] *Peng, S.T.* **"Transitions in open millimetre-wave waveguides"** Microwaves, Antennas and Propagation [see also IEE Proceedings-Microwaves, Antennas and Propagation], IEE Proceedings H , Volume: 136 , Issue: 6 , Dec. 1989 Pages: 487 − 491

[8] *Shanjio Xu; Peng, S.T.; Schwering, F.K.* **"Effect of transition waveguides on dielectric waveguide directional couplers"** Microwave Theory and Techniques, IEEE Transactions on , Volume: 37 , Issue: 4 , April 1989 , Pages: 686 − 690

[9] *Xu, S.-J.* **"Dielectric-waveguide branching directional coupler"** Microwaves, Antennas and Propagation , IEE Proceedings H , Volume: 135 , Issue: 4 , Aug. 1988 , Pages: 282 - 284

[10] *Altschuler, H.M.; Goldstone, L.O.* **"On Network Representations of Certain Obstacles in Waveguide Regions"** Microwave Theory and Techniques, IEEE Transactions on , Volume: 7 , Issue: 2 , Apr 1959 , Pages: 213 − 221